WARSAW UNIVERSITY OF TECHNOLOGY Index 351733
FACULTY OF CIVIL ENGINEERING
COMMITTEE FOR CIVIL AND WATER ENGINEERING
POLISH ACADEMY OF SCIENCES ISSN 1230-2945

DOI: 10.24425/ace.2021.137169

ARCHIVES OF CIVIL ENGINEERING

Vol. LXVII ISSUE 2 2021

s. 293–307



**Case study**

# Analysis of the behaviour of the high and steep slope of a road made through waste under the influence of rainfall

**E. Pilecka[1], J. Zięba[2], D. Szwarkowski[3]**

**Abstract:** Investments in made ground are a big problem. The present investigation concerns ground derived from limestone treatment waste from SOLVAY soda plants. This waste is deposited in the southern area of Krakow in a reservoir called 'White Seas' in an area of approximately 15 ha. Currently, part of the route and tram investment, 'The Łagiewniki Route' Currently through the 'White Seas' area. The article presents an analysis of a section of this route by a high and steep slope made from made ground. The first stage of the in-situ measurements was to scan the shape of the high slope with the RIEGL VZ-400 terrestrial laser scanner. It was necessary to obtain the shape of the slope for numerical modelling using the FEM method. The point cloud perfectly reflected the shape of the slope with an accuracy of 5 mm. Soil samples (limestone waste) were also collected in the area of the slope for laboratory tests. In order to determine the effective strength parameters of the made ground of the embankment, a series of tests was carried out using triaxial compression apparatus. All triaxial tests were performed in accordance with British Standard 1337 Part 8. Modelling was performed using an FEM finite element method in MIDAS. The analyses also included the variant of irrigation of made ground. The conducted research shows that the high and steep slope made from calcareous waste indicates stability. The irrigated land did not make the high escarpment unstable.

**Keywords:** triaxial test, slope stability, FEM

[1] DSc., PhD., Eng., Prof. of CUT, Cracow University of Technology, Faculty of Civil Engineering, ul. Warszawska 24, 31-155 Kraków, Poland, e-mail: epilecka@pk.edu.pl, ORCID: https://orcid.org/0000-0002-1536-4291

[2] MSc., Eng., Cracow University of Technology, Faculty of Civil Engineering, ul. Warszawska 24, 31-155 Kraków, Poland, e-mail: jzieba@pk.edu.pl, ORCID: https://orcid.org/0000-0002-9252-296X

[3] MSc., Eng., Cracow University of Technology, Faculty of Civil Engineering, ul. Warszawska 24, 31-155 Kraków, Poland, e-mail: dszwarkowski@pk.edu.pl, https://orcid.org/0000-0002-8925-778X

# 1. Introduction

One of the results of human activity is made ground. In most cases, such areas of ground are produced by industry. The physical parameters of such ground are varied, but they are often used in civil engineering. At present in Poland, there are several proposed road investments where the planned roads are to be located on made ground. One of these is located in the south of Krakow and is called ‘Trasa Łagiewnicka’. This article focuses on the longest tunnel on the ‘Trasa Łagiewnicka’ which is located in the area of the so-called ‘White Seas’ (Fig. 1).

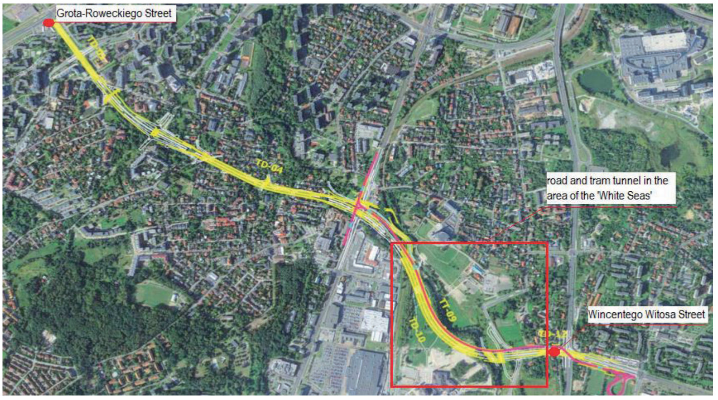


Fig. 1 Location of the Łagiewnicka route with an outline of the ‘White Seas’ area [17]

The construction of the road started in 2018, and it is a part of the future Krakow ring road [10]. The total length of the road is 3.5 km and 2 km of this road is to be located below ground level. The longest tunnel on the route is located in the ‘White Seas’ area. ‘White Seas’ is a place where calcareous waste from the soda factory ‘Solvay’ in Krakow was stored [5]. Due to the fact that 57% of the ‘Łagiewnicka Route’ is located below ground level and a considerable part of the route is located on made ground, it is anticipated that several geotechnical engineering problems will be encountered in the construction of the future Krakow ring road. Due to the nature of the investment (complex geology, properties of the made grounds of the ‘White Seas’, the construction technology of the tunnel using the excavation method), it is important to properly design and monitor the excavation high and steep slopes.

## 2. In-situ area measurement

Measurements with a terrestrial laser scanner are widely used in the analysis of slopes, particularly in the case of slopes with active landslides [2], [18]. The article discusses the use of measurements obtained with a Riegl VZ 400 laser scanner to build a numerical model. Measurement with the device involves the construction of a test site covering the area of research. The number of research points depends on the sampling frequency of the device and the scaling range. In the case of the Riegl VZ 400 scanner, the measurement points are located at distances no greater than 400 m apart. This made it possible to obtain a measuring accuracy of 5 mm. The scanning process itself is automatic. A combination of frame and linear scanning is used, on the basis of which, a point cloud is created from each measuring point [12].

This article focuses on a stability analysis of the existing deep excavation slopes using an in-situ method based on terrestrial laser scanner measurements and a determination of the stability factor based on the SRM method and using the finite element method. The obtained results made it possible to compare the current slope stability during the period of the measurements and the calibration of the parameter values entered into the numerical model. On this basis, a possible deterioration in the stability factor of the slopes as a result of precipitation and due to the use of the terrain surface was indicated by measurements performed with a terrain laser scanner.

In the next part of the article, the part of the slope with the highest height and the smallest slope (Fig. 2) is analysed. The numerical simulation of the analysed part of the excavation takes into account the daily rainfall and measurements of deformation of the slope with a terrestrial laser scanner. The analysed part is shown in Figs. 3 A, and 3 B. The total height of the analysed slope was 20 m.

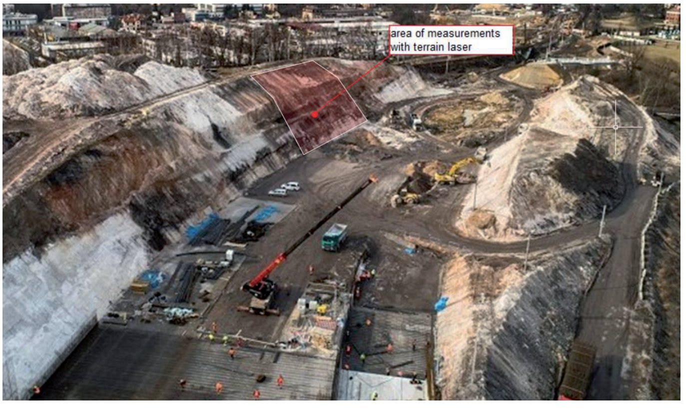


Fig. 2 Study area and numerical tested region [17]

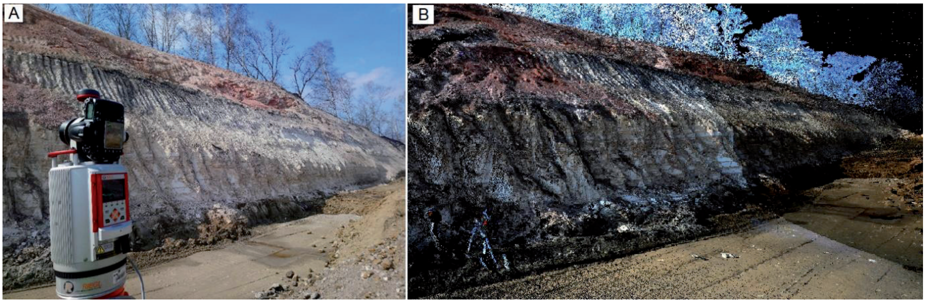


Fig. 3A Image of the excavation works with the terrestrial laser scanner position;
3B Results data from the terrestrial laser scanner

## 3. Laboratory test

The tests for determining the effective strength parameters of made ground were performed using VJ-Tech triaxial compression apparatus [6, 7, 8]. All laboratory CD Triaxial compression tests were conducted according to British Standard 1337 Part 8. This part of BS 1377 specifies the procedures for the determination of the effective shear strength parameters of the tested samples [3]. The specimens were saturated using a back pressure method. In this method, 50 kPa increments of cell pressure and back pressure are applied alternately. Full saturation was checked with the use of the B-Skempton pore water pressure coefficient, which is defined as the ratio between the pore water pressure variation and the mean total stress variation when isotropic compression is performed in undrained conditions. For all samples, a full-saturation condition is reached when the cell pressure is between 300 and 400 kPa. The main goal of the next step, which is the isotropic consolidation stage, is reached by confining the effective stress in the tested sample. During the consolidation stage, changes in the pore water pressure and the volume of the specimen were recorded. Specimens were isotropically compressed until the pressure in the sample was fully dissipated. The final stage of the triaxial test was compression in a drained condition. For this stage, cell and back pressure were maintained. For all tests, a frame speed range of between 0.005-0.008 [mm/min] was adopted. During the shearing stage, no increase in pore water pressure was noted. The results of compressing the samples in a triaxial cell is the axial stress versus axial strain presented in Figs. 4A and 4B.

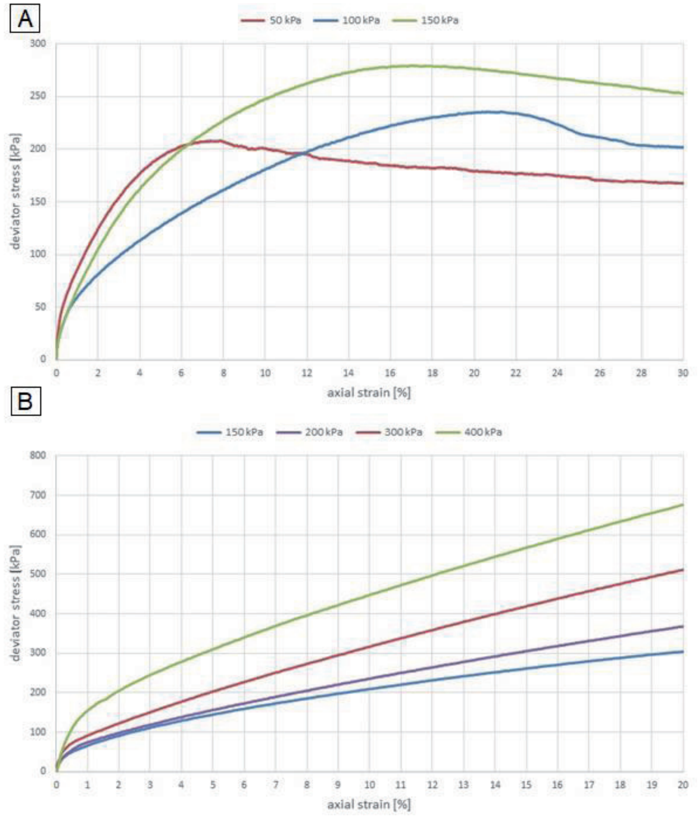


Fig. 4A Stress-strain curve for samples from 5 m b.g.l.; 4B Stress-strain curve for samples from 15 m b.g.l., deviator stress q [kPa] versus axial strain εa [%];

Consolidation curves are presented in Figs. 5A and 5B. The secant moduli of the deformation curves are presented in Figs. 6A and 6B. The effective stress path method [16] (MIT diagram) was used for determining the shear strength parameters and t-s plots are presented on Figs. 7A and 7B. Finally, based on the results, the effective friction of angle and effective cohesion were determined. The results for ground samples for 5 m below ground level (b.g.l.) are presented in Figs. 4A, 5A, 6A and 7A; for 15 m b.g.l., results are presented in Figs. 4B, 5B, 6B and 7B.

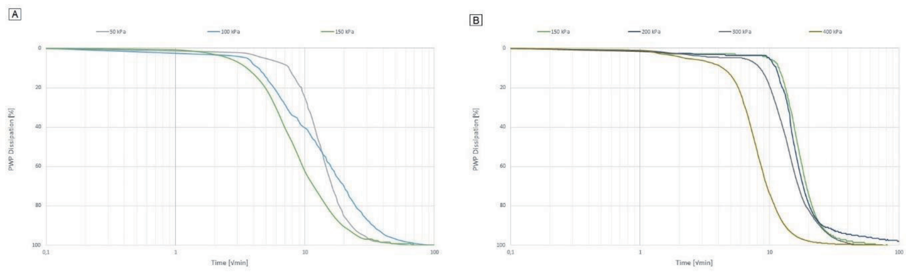


Fig. 5A Consolidation curve for samples from 5 m b.g.l.; 5B Consolidation curve for samples from 15 m b.g.l.

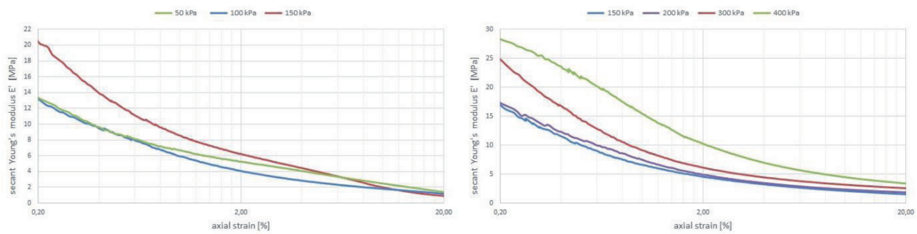


Fig. 6A The secant moduli of deformation for samples from 5 m b.g.l.; 6B The secant moduli of deformation for samples from 15 m b.g.l.

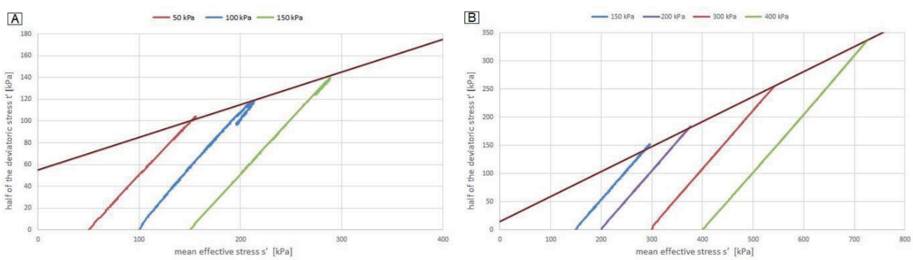


Fig. 7A Stress path parameters, s' and t' [kPa], for samples from 5 m b.g.l.; 7B Stress path parameters, s' and t' [kPa], for samples from 15 m b.g.l.

For further calculations based on triaxial test results, the following parameters were determined:

- filtration coefficient k [m/s]
- effective friction angle φ' [deg]
- effective cohesion c' [kPa]
- secant modulus of deformation E [MPa]

# 4. Numerical model - present ground conditions

The results obtained from in-situ analyses with a terrestrial laser scanner and laboratory tests enabled the calibration of a numerical model of the analysed area of the excavation slope. Numerical analysis allows the determination of slope stability. Table 1 shows the material physical parameters from the laboratory testing of ground which were used in numerical the analysis. The most unfavourable parameter values were adopted.

Table 1. Ground physical parameters used in the numerical calculation

| Ground type | Bulk density [g/cm$^3$] | $I_L/I_D$ | $e_0$ | $S_r$ | k [m/s] | v [-] | φ' [°] | c' [kPa] | $E_0$ [kPa] |
|---|---|---|---|---|---|---|---|---|---|
| Sediment I | 1.10 | - | 4.90 | - | $10^{-5}$ | 0.35 | 21.36 | 12 | 25,000 |
| Sediment II | 1.20 | - | 1.43 | - | $10^{-5}$ | 0.35 | 14.4 | 44 | 25,000 |
| sasiCl | 2.05 | 0.15 | 0.57 | 0.35 | $10^{-8}$ | 0.30 | 12.10 | 19.20 | 12,600 |
| MSa | 2.00 | 0.50 | 0.62 | 0.36 | $10^{-3}$ | 0.30 | 27.45 | 0 | 41,500 |
| saGr | 2.10 | 0.70 | 0.44 | 0.32 | $10^{-3}$ | 0.30 | 32.94 | 0 | 121,500 |
| Cl | 2.00 | 0.00 | 0.62 | 0.31 | $10^{-11}$ | 0.30 | 32.01 | 23.2 | 25,000 |

Slope stability was calculated using a 3-D FEM model. For a better presentation of the slip surface, the results of numerical calculations are also presented in a 2D cross section. The elastic-plastic behaviour of the considered ground was taken into account. The generalised Coulomb-Mohr failure criterion was used to determine the strength parameters of the ground mass.

(3.1) $$f = |\tau| + \sigma_n tan\varphi - c = 0$$

where:

$\tau$ – shear stress [Pa], $\sigma_n$ – main normal stress [Pa], $\varphi$ –internal soil friction angle [deg], c -cohesion [Pa]

Data from the terrestrial scanner was appropriate for creating a reliable digital surface model. The tetrahedral elements were used for the discretisation of the numerical model (Fig. 8). A finite element size of 0.25 m was used near the edge of the slope. The shear strength reduction method (SRM) was used to determine the slope stability factor of the existing slope. The value of the safety factors was determined in accordance with the D.A.3 approach proposed in PN-EN 1997-1: 2008 [13].

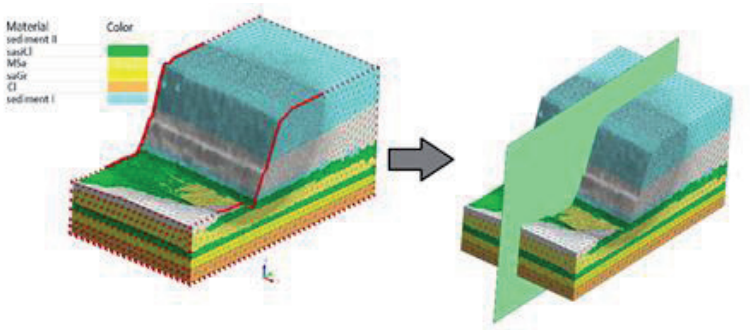


Fig. 8 Slope numerical model 3D and cross section 2D

## 5. Numerical model - prognosis

Calcareous sediments were separated into two layers because of the porosity and water content. The porosity of the first layer (0-15 m deep) is 83% and the water content is around 150%. Below the first layer, the porosity calcareous sediments were at the lower level of 59% (15-22 m) and the water content decreased to 100%. However, the degree of saturation in both of the calcareous layers is between 85 and 95%. All physical properties of the soil (water content, bulk density and void ratio) were determined according to PN ISO 17892 [4].

Due to the significant height of the slope (20 m height and a slope of less than 1:1), which is included in the analysis of both the differential and numerical model, additional numerical simulations were conducted. A water flow analysis was performed, taking into account the transient analysis with changing water conditions related to the inflow and outflow of rainwater.

Additional numerical analyses made it possible to determine the influence of rain factors on the behaviour of the slope. The numerical analysis took into account the behaviour of ground that was not fully saturated (the possibility of drying subsurface layers of calcareous sediments was included in the calculations).

The behaviour of the medium which was not fully hydrated and the change in the value of the filtration coefficient were determined on the basis of a numerical simulation taking into account the change in the porosity index Δe in the flow analysis based on the initial value $e_0$. The function $k_r = k_r$ (p) was used, this was determined for the ground which was waterlogged according to Darcy's law ($k_{sat}$). The permeability coefficient ($c_k$) of the layer depends on the change in the porosity index Δe and may be determined from equation (2) [9]:

(5.1) $$k = 10^{\frac{\Delta e}{c_k}} k_r(p) k_{sat}$$

In order to determine the changes in the value of the filtration coefficient over time related to the change in the porosity of the calcareous layers, the van Genuchten formula was used for ground which was not fully saturated [1]. The following permeability coefficient formula can be used.

(5.2) $$k_r = \frac{\left[1-(ah)^{n-1}((1+(ah)^n)^{-m})\right]^2}{[1+(ah)^n]^{\frac{m}{2}}}$$

where:

a, n, m are curve fitting parameters, m = 1-1/n

Seepage analysis generally uses the volumetric water content, which is the ratio between the total volume and water volume. The van Genuchten function can be used to compute the volumetric water content.

(5.3) $$\theta = \theta_r + \frac{\theta_s - \theta_r}{(1+(a\bar{p})^n)^m}$$

where:

$\theta_r$ - minimum volumetric water content, $\theta_s$ - maximum volumetric water content, a, n, m - are curve fitting parameters, m = 1-1/n

The value of the van Genuchten-Mualem model (VGM) coefficients was determined based on the pedotransfer analytical model, using the percentage of fractions obtained from a granulometric analysis. The parameters obtained for the numerical model are presented below in Table 2.

Table 2 Parameters of the van Genuchtena-Mualema model used in the numerical analysis

| Parameters used in the numerical analysis | | | |
|---|---|---|---|
| Type of material: | | Sediment I | Sediment II |
| Total water content | $Q_S$ | 0.499 | 0.470 |
| Residual woter content | *$Q_R$ | 0.015 | 0.015 |
| VGM model parameter | a | 0.167 | 0.128 |
| VGM model parameter | n | 1.01 | 1.01 |

* Parameter with a negligible impact on the van Genuchtena-Mualema model (Rossi, Nimmo 1994, Haverkamp in. 2005 [11], [15] some researchers use the value 0)

The changes in the properties of calcareous sediments subjected to weather conditions were based on statistics obtained from the statistical offices in Krakow. The rainfall statistics covered the period between 18.10.2018 and 19.03.2019 (Fig. 9) when there were no construction works on the slope. After 19th March 2019, the tunnel lining was built in the excavation and the channel formed by the slopes was filled in.

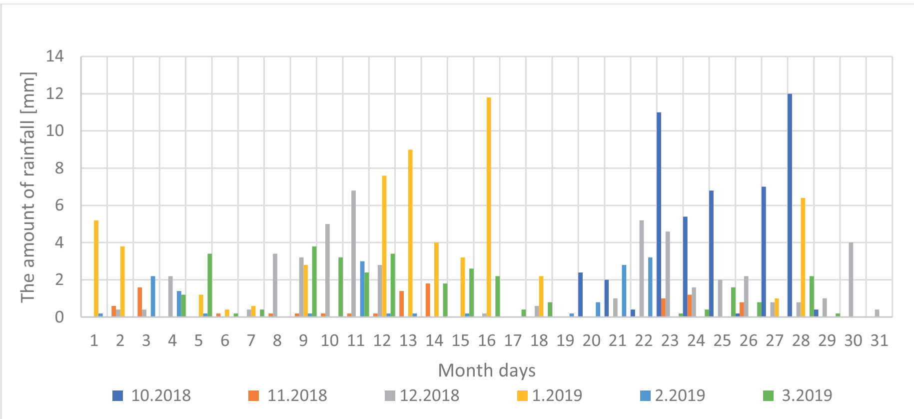


Fig. 9 Daily rainfall in Krakow in the period from October 2018 to March 2019

Daily rainfall in Krakow in the period from 10.2018 to 3.2019 was used to define the 'surface flux' in the tested model. As a result, the rainfall data was used to create a time-dependent function, which is presented in Fig. 10.

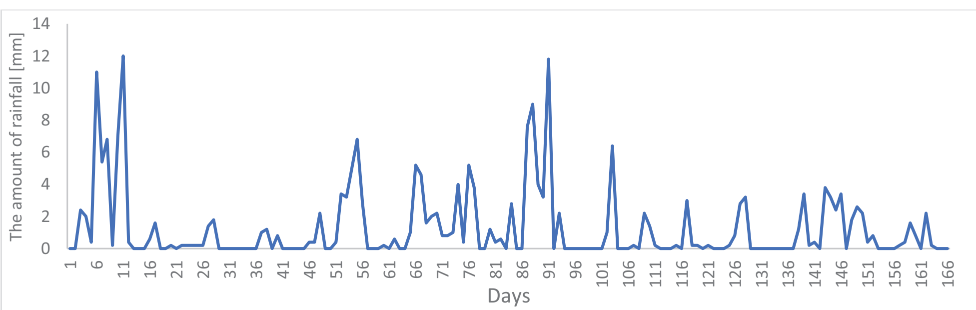


Fig. 10 The surface flux functions used in numerical analysis

## 6. Results

As a result of data processing and calculation, the results described below were obtained (Fig. 11). The result of the global stability analysis, with the use of in-situ parameters, shows that the slope is in a state of equilibrium. A factor of safety FoS value of 1.07 was obtained. The global slope stability parameter was determined on the basis of the assumptions given in Eurocode 7, which characterises the slope as stable.

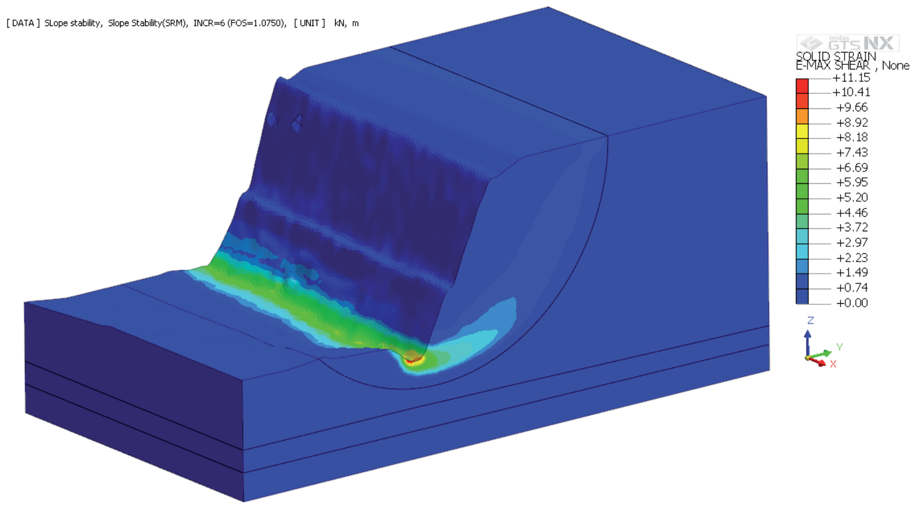


Fig. 11 The result of the global stability analysis of the slope in 3D, FoS = 1.07

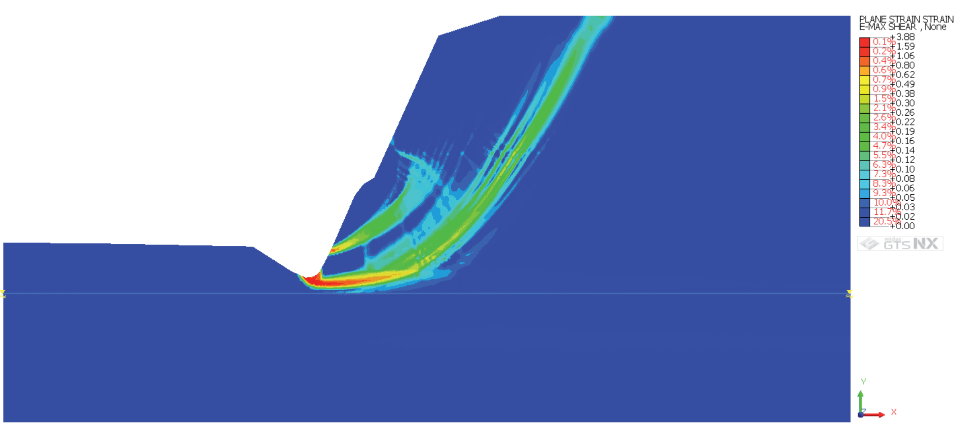


Fig. 12 The result of the global stability analysis of the slope in 2D, FoS= 1.07

In the presented cross section, two slip zones are clearly visible, one deep below the ground surface, the other from the side of the slope in the middle of the cross section. The slope subjected to atmospheric precipitation was also analysed in the period between October 2018 and March 2019. Figure 13 presents the form of loss of stability of the analysed slope of the 'White Seas' calcareous waste deposit .

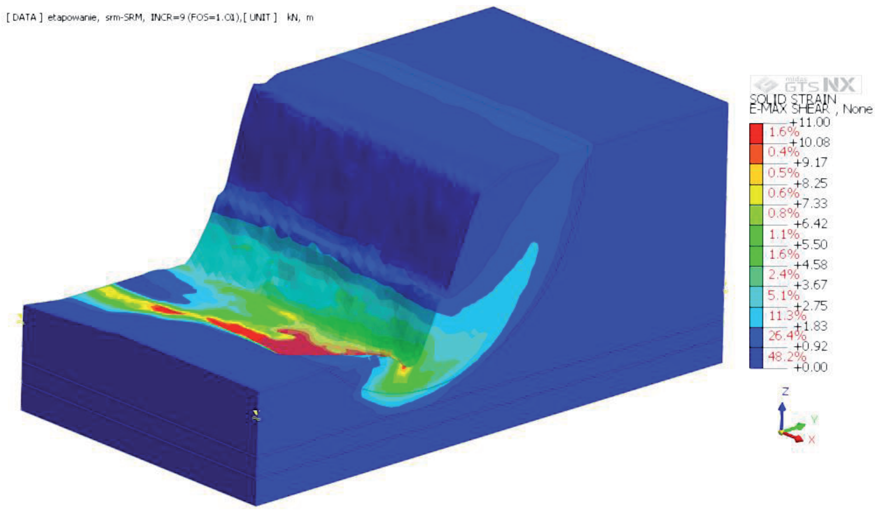


Fig. 13 The result of the global stability analysis of the slope in rainy conditions in 3D, FoS= 1.01

For a more detailed analysis of the slip surface, the model is presented as a cross section (Fig. 14).

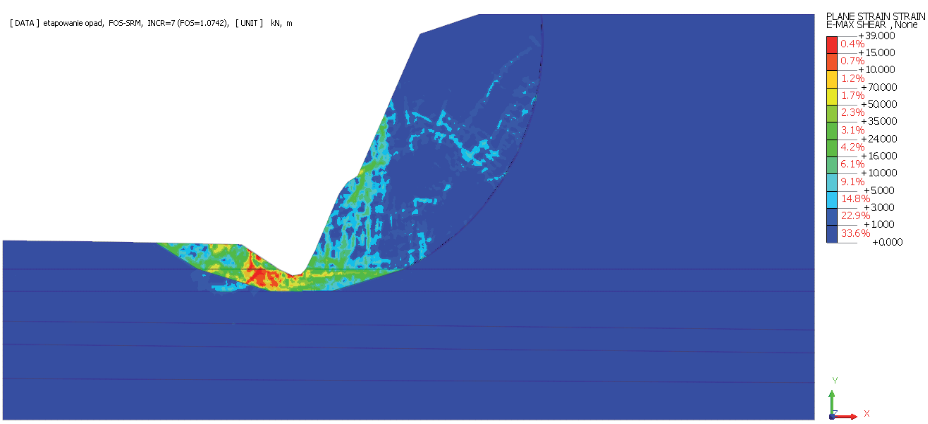


Fig. 14 The result of the global stability analysis of the slope in rainy conditions in 2D, FoS= 1.01

Numerical analysis of the calcareous waste irrigated by rainfall in the period between 18th October 2018 and 19th March 2019 showed the limit value of slope stability. The results are at the limit of stability at FoS= 1 (Fig. 13). In the case of non-hydrated waste, the obtained value of the safety factor was FoS = 1.07. This is the larger value, but the stability value is nevertheless close to the limit value of FoS = 1. On the basis of Eurocode 7, design parameters DA3 were adopted, the value of the stability coefficient is greater than or equal to one (FoS ≥1) and the slope is stable. It is also interesting to obtain the results in the form of a slip plane. In the case of a high slope of the analysed waste, the slip plane is clearly marked in the initial conditions. In the case of irrigated grounds, the slip plane is not clearly marked, it is blurred. The properties of these analysed lime waste probably result in the lack of a more pronounced slip surface and the obtained safety factor after irrigation.

## 6. Conclusions

Numerical simulations took the initial conditions into account, the terrestrial scan data and the rainfall conditions of the slope made from calcareous ground confirmed the stability of the slope. The terrestrial laser scanner provided excellent information on the slope geometry. Despite the depth of the excavation (20 m) and the inclination in some places being less than 1: 1, the considered slopes are stable. The influence of rainfall conditions is negligible and can only cause surface run-off of the anthropogenic material. However, the slope stability should be approached with caution because the stability coefficients are close to FoS = 1.07. However, it should be remembered that the value of the coefficient of FoS = 1.07 has a small safety margin. In road construction in Poland, the value of the stability coefficient is assumed to be equal to or greater than 1.5 (Fos ≥ 1.5) [18]. According to Eurocode 7, a lower but safe value can be assumed, which is to be determined by the designer. In the irrigated ground variant, the stability coefficient is slightly lower than that of the non-watered variant. Numerical analysis provided information on the behaviour of a high and steep slope comprised of calcareous waste. Such information should be obtained prior to construction works. This would allow assessment of the risk of stability of such a slope under the influence of irrigation from rain.

## References

[1] MT. Van Genuchten, “A close-from equation for predicting the hydraulic conductivity of unsaturated soils”, Soil Science Society of America Journal, vol. 44, issue 5, pp. 892-898, Sep. 1980. https://doi.org/10.2136/sssaj1980.03615995004400050002x

[2] J. Kogut, E.Pilecka, D. Szwarkowski, "Analysis of landslide effects along a road located in the Carpathian flysch”, Open Geosciences, vol. 10, issue 1, pp.517–531, Sep. 2018. https://doi.org/10.1515/geo-2018-0041

[3] BS EN 1337-8:2007 Structural bearings. Guide bearings and restraint bearings.

[4] EN ISO 17892 Geotechnical investigation and testing - Laboratory testing of soil.
[5] W. Sroczyński, "Geological condition of revitalization and land development the "BiałeMorza" on the terrain safter former "Solvay" Krakow Soda Works, GEOLOGIA, Urząd Miasta Krakowa, vol. 34, issue 4, pp. 701–709, 2008.
[6] U. Smoltczyk, "Geotechnical Engineering Handbook", Ernst & Sohn Verlag, 2002.
[7] L.D. Wesley, "Geotechnical Engineering in Residual Soils", John Wiley & Sons, Inc., 2010.
[8] B. Wrana, "Lectures on soil mechanics, Wydawnictwo PK, Kraków, 2014.
[9] MIDAS GTS NX, "Manual specifications", 2019.
[10] I. Kupiec, P. Mleczko, "Miejscowy plan zagospodarowania przestrzennego obszaru „Białe Morza" prognoza oddziaływania na środowisko. Urząd miasta Krakowa biuro planowania przestrzennego pracownia branżowa, Kraków, 2012.
[11] C. Rossi, JR. Nimmo, "Modeling of soil water retention from saturation to oven dryness", Water Resources Research, vol. 30, no. 3, pp. 701-708, March 1994. https://doi.org/10.1029/93WR03238
[12] RIEGL LMS, "Oprogramowanie Systemowe i Przetwarzania Danych RiSCAN PRO dla skanerów laserowych 3D firmy RIEGL LMS", Austria, 2009.
[13] Polska Norma PN-EN-1997-2 Eurokod 7. Projektowanie geotechniczne. Część 2: Rozpoznanie i badanie podłoża gruntowego.
[14] Rozporządzenie Ministra Transportu i Gospodarki Morskiej z dnia 2 marca 1999 r. w sprawie warunków technicznych, jakim powinny odpowiadać drogi publiczne i ich usytuowanie (Dz. U. 1999 nr 43 poz. 430).
[15] F.J. Leij, R. Haverkamp, C. Fuentes, F. Zatarain, P.J. Ross, "Soil Water Retention", Soil Science Society of America Journal, vol. 69, issue 6, pp. 1891-1901, Nov. 2005. https://doi.org/10.2136/sssaj2004.0226
[16] P. V. Lade, "Triaxial Testing of Soils", Wiley Blackwell International Commission of Large Dams, Oxford, 2016.
[17] www.trasalagiewnicka.krakow.pl.
[18] M. Cała et all, „Wytyczne do oceny stateczności skarp nasypów i wykopów w szczególnych warunkach geologiczno-inżynierskich, a także przy wykonywaniu budowli drogowych na terenach górniczych", AGH, Kraków 2018.

## Analiza zachowania wysokiej i stromej skarpy zbudowanej z gruntów odpadowych w inwestycji transportowej

Słowa kluczowe: testy w aparacie tójosiowego ściskania, stateczność skarpy, MES

### Streszczenie:

W artykule przedstawiono interesujący problem geotechniczny jaki wystąpił w trakcie realizowania inwestycji na gruntach odpadowych. Inwestycja wymagała wykonania głębokiego wykopu w gruntach odpadowych. Powstała wysoka skarpa 20 metrowa. Z uwagi na ciekawy problem geotechniczny podjęto prace badawcze in-situ i laboratoryjne w celu określenia parametrów geotechnicznych tych odpadów i analizy stateczności wysokiej skarpy. Grunty odpadowe są z reguły mają skomplikowane, różnorodne właściwości i mogą być trudne dla budownictwa. Aktualnie w realizowanych inwestycjach można spotkać się z taką sytuację, że konieczne jest budowanie na takich gruntach. Taka sytuacja zaistniała na Trasie Łagiewnickiej. Trasa Łagiewnicka to obecnie budowana od 2018 roku południowa obwodnica Krakowa. Projektowana trasa o łącznej długości 3,5 km, przeprowadzona zostanie na odcinku 2 km w tunelach. Najdłuższy odcinek tunelu wybudowany zostanie w rejonie tzw. Białych Mórz, zbiornika odpadów z przeróbki wapnienia w zakładach sodowych SOLVEY.

W celu utworzenia rzeczywistego modelu wysokiej skarpy zastosowano nowoczesną metodę teledetekcji naziemnym skanerem laserowym RIEGL VZ-400. Pomiar tym urządzeniem polega na wykonaniu poligonu badawczego obejmującego zasięgiem obszar badań. Otrzymanym rezultatem jest „chmura" punktów odzwierciedlająca rzeczywistą geometrię wysokiej skarpy z dokładnością do 5mm. Taki model został zastosowany do modelowania FEM.

Odrębnym zagadnieniem było pobranie próbek gruntu odpadowego w analizowanym miejscu i badania laboratoryjne ich parametrów geotechnicznych. Grunty antropogeniczne mogą wykazywać zupełnie odmienne właściwości od gruntów ogólnie znanych. Dlatego tak ważne jest wykonanie badań laboratoryjnych potrzebnych do modelowania numerycznego FEM. W celu określenia efektywnych parametrów wytrzymałościowych gruntu nasypu antropogenicznego wykonano

serię badań z wykorzystaniem aparatu trójosiowego ściskania. Wszystkie badania trójosiowe zostały przeprowadzone zgodnie z normą British Standard 1337 Part 8. Na podstawie wyników ścinania w aparacie trójosiowego ściskania została przeprowadzona analiza w celu określenia parametrów wytrzymałościowych.

Uzyskane wyniki z analiz in-situ naziemnym skanerem laserowym i badania laboratoryjne pozwoliły skalibrować model numeryczny analizowanego obszaru skarpy wykopu. Obliczenia przeprowadzono metodą elementów skończonych w programie MIDAS. Uwzględniono sprężysto-plastyczne zachowanie rozpatrywanego ośrodka gruntowego. Przyjęto model gruntu bazujący na hipotezie wytężeniowej Coulomba-Mohra. W celu wyznaczenia wskaźnika stateczności (zapasu bezpieczeństwa) istniejącej skarpy wykorzystano metodę redukcji wytrzymałości na ścinanie (SRM). W wyniku przeprowadzonych analiz numerycznych na wartościach początkowych parametrów geotechnicznych warstw, uzyskano następującą wartość wskaźnika stateczności F=1,07. Wyznaczony parametr stateczności globalnej skarpy na podstawie założeń podanych w Eurokodzie 7 charakteryzuje skarpę jako stateczną. Potwierdza to obserwacje prowadzone na terenie budowy. W celu uzyskania prognozy stateczności skarpy z gruntu odpadowego nawodnionego przeprowadzono drugie symulacje numeryczne. W celu określenia zmian w wartości współczynnika filtracji w czasie związanym ze zmianą porowatości warstwy geotechnicznej zastosowano wzór van Genuchtena dla gruntów nie w pełni nasyconych. Analiza numeryczne skarpy nawodnionej wykazała współczynnik stateczności F=1,01. Niemniej jednak wartość stateczności jest bliska granicznej wielkości F=1. Interesujące jest także uzyskanie wyników w postaci płaszczyzny poślizgu. W przypadku skarpy wysokiej z analizowanych gruntów odpadowych w warunkach początkowych jest ona wyraźnie zaznaczona. A w przypadku gruntów nawodnionych płaszczyzna poślizgu nie jest wyraźnie zaznaczona, jest rozmyta. Poruszony w artykule problem inwestycji w gruntach odpadowych jest niezwykle ważny z punktu widzenia inżynierskiego.

Received: 16.10.2020, Revised: 05.01.2021